Numerical Simulation of the Flow Excited Acoustic Resonance of Two Tandem Cylinders in Cross-Flow

Atef Mohany[1] and Samir Ziada
Department of Mechanical Engineering, McMaster University, Hamilton, Canada
[1]*Current address: Atomic Energy of Canada Limited, Chalk River Laboratories, Canada*

ABSTRACT

This paper presents a numerical simulation of the flow-excited acoustic resonance for a single cylinder and two tandem cylinders in cross-flow. The simulation Reynolds number is 25000 and the spacing ratio of the tandem cylinders is 2.5. Howe's theory of aerodynamic sound is used to reveal the details of the aeroacoustic sources in the flow field. In the single cylinder case, the excitation source is located in the cylinder near wake. For the case of two tandem cylinders, two aeroacoustic sources are identified. The first is located in the near wake of the downstream cylinder and is found to be the primary source exciting the coincidence acoustic resonance. The second aeroacoustic source is located in the gap between the cylinders and is shown to be the main excitation source of the precoincidence acoustic resonance.

1. INTRODUCTION

The flow-excited acoustic resonance phenomenon, where the flow surrounding a bluff body vibrates in a resonant manner, is a design concern in many engineering applications such as tube bundles of heat exchangers, boiler plants, turbomachines, piping systems, and reactor vessels. It causes noise and vibration problems and could lead to fatigue failure to the equipment. This is because when these resonances are excited, the resulting acoustic pressure may exceed the dynamic head of the mean flow. A crucial event in the mechanism of acoustic resonance is the ability of sound to modulate, and essentially "lock-in", the process of vortex shedding. While this phenomenon is relatively well understood for the case of *isolated* cylinders, Blevins (1985), there are many unresolved issues for the more complex case of multiple cylinders in close proximity.

A recent study by Mohany and Ziada (2005) has shown that the aeroacoustic response of two-tandem cylinders in cross-flow can be considerably different from that of a single cylinder under similar flow conditions. In the tandem cylinders case, strong resonance of a given mode occurs over two different ranges of flow velocity, a coincidence resonance which occurs near the velocity of frequency coincidence and the precoincidence resonance which occurs at a substantially lower flow velocity. This is in contrast with the single cylinder case for which the resonance occurs over a single velocity range. Moreover, it has been suggested that the coincidence resonance in the tandem cylinders case is excited by vortex shedding in the downstream wake, whereas the pre-coincidence resonance is excited by the flow instability in the gap between the cylinders. In this paper, a numerical simulation is performed to examine this supposition. The objective is to reveal the nature and the locations of the aeroacoustic sources causing the pre-coincidence and the coincidence resonances and compare the results with those of the single cylinder case.

Hourigan et al. (1986) performed a numerical simulation of the flow-induced acoustic resonance for a plate in a duct. They used Howe's theory of aerodynamic sound (Howe 1975, 1984) to identify the aeroacoustic sources in the flow field. They found the primary aeroacoustic source to be in the region at the trailing edge of the plate. Stoneman et al. (1988) investigated the acoustic resonance generated by flow over two plates in the tandem arrangement. By means of numerical simulations, they were able to show that the net energy transfer between the flow and the sound field is dependent on the spacing between the plates. Moreover, they observed the existence of a net acoustic source in the trailing edge region of the upstream plate during resonance. However, in the wake region of the downstream plate, there was either an acoustic source or a sink, depending on the phasing between the flow activities during the acoustic cycle

Hourigan et al. (1990) investigated experimentally and numerically the aerodynamic sources of acoustic resonance in a duct with two baffles. The resonant longitudinal acoustic mode was calculated using a finite element method and the flow field was predicted using a discrete-vortex model. The acoustic energy generation was predicted by means of Howe's theory of aerodynamic sound.

More recently, Tan et al. (2003) investigated the flow-excited acoustic resonance of rectangular plates in a duct. They accounted for the effect of the acoustic field by applying, in the transverse direction, an oscillatory velocity perturbation at the inlet and the side boundaries. The main advantage of using this technique is that the flow velocities at which acoustic resonance occurs can be predicted

In this paper, a numerical simulation of the flow-sound interaction mechanisms is performed for the case of a single and two tandem cylinders in cross-flow. For the case of two tandem cylinders, only one spacing ratio, which is inside the proximity interference region, was considered, L/D = 2.5, where L is the centre-to-centre distance between the cylinders and D is the cylinder diameter.

2. NUMERICAL TECHNIQUE

First, the flow field and the sound field are simulated separately (i.e. uncoupled). In order to simulate the coupling phenomenon, the simulation of the unsteady flow field was repeated with applying an oscillatory transverse velocity perturbation, which simulates the acoustic particle velocity of the resonant sound field.

The acoustic sources (or sinks) in the flow field are then predicted by combining the solution of the acoustic field, which is modeled by the finite-element method using ABAQUS, with the acoustically forced unsteady flow field, which is modeled using the Spalart-Allmaras (S-A) turbulent model in FLUENT. The instantaneous sound power P generated by the convection of unsteady vorticity within a sound field was calculated from Howe's theory of aerodynamic sound (1975, 1984):

$$P = -\rho \int \vec{\omega} \cdot (\vec{u} \times \vec{v}) d\forall \qquad (1),$$

where $\vec{\omega}$ is the vorticity vector, $\vec{u}$ is the flow velocity vector and $\vec{v}$ is the acoustic velocity vector. The net acoustic energy is the integration of the instantaneous acoustic power over a complete acoustic cycle. Therefore, the locations within the flow field where the acoustic energy is either absorbed or generated can be identified.

3. SINGLE CYLINDER RESULTS

3.1 Flow Field

The simulation of the flow field was performed at a Reynolds number of 25000 using the S-A turbulent model in FLUENT. Despite the relatively high Reynolds number, the flow is assumed two-dimensional because previous experiments have shown that during acoustic resonance the flow becomes two-dimensional. The flow parameters at this Reynolds number are as follows: the mean flow velocity is 28.75 *m/s*; the cylinder diameter is 12.7 *mm*; the working medium is air with a density of $\rho = 1.225$ *kg/m*^{3}, and a viscosity of $\mu = 1.7894\times10^{-5}$ *kg/m.s*. The simulation boundaries are placed at ± 10D in the cross-flow direction, 20D upstream and 40D downstream of the cylinder. Unstructured triangular mesh was used with a 66770 triangular cells. The smallest grid size is about 8.339×10^{-5} *m*. Segregated (implicit) solver with a second-order discretization scheme was used throughout this simulation. For the velocity-pressure coupling, SIMPLEC algorithm was used. The time step size used for the computation is 5×10^{-5} *sec*, which means that each vortex shedding cycle was simulated in 40 time steps.

The lift and the drag force coefficients, as well as the wake pattern before applying the cross-flow oscillation are shown in figures 1 and 2, respectively. The mean drag force coefficient is about 1.03, and the r.m.s lift coefficient is about 0.61. The lift coefficient is slightly higher than that measured in the experiments, Mohany (2006), because the flow is assumed two-dimensional in the present simulation. The calculated Strouhal number based on the cylinder diameter is 0.215. The simulation results agree also with those reported by Saghafian et al. (2003). They simulated the flow around a circular cylinder using nonlinear eddy-viscosity modeling. At a Reynolds number of 25000, Saghafian et al. (2003) reported a mean drag coefficient of 1.15, r.m.s. lift coefficient of 0.5; and a Strouhal number of 0.225.

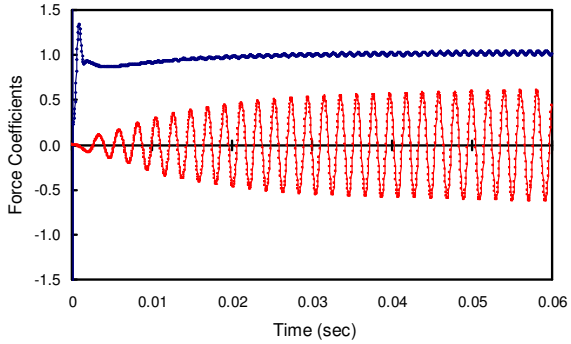

Figure 1: Drag and lift coefficients for a single cylinder at Re = 25000, no acoustic excitation.

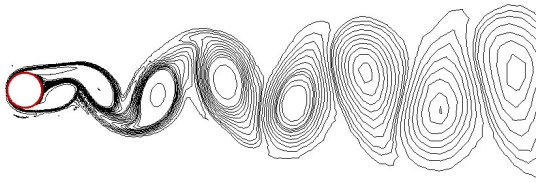

Figure 2: Vorticity contours behind the single cylinder at Re = 25000.

3.2 Acoustic Field

A numerical simulation was performed to model

the resonant sound field with the aid of the finite-element analysis in ABAQUS. The acoustic modes in the duct housing the cylinder exhibit simple harmonic oscillations. Therefore, the acoustic pressure of the resonant mode can be expressed as $p = \phi e^{i(2\pi f)t}$, where ϕ is a function satisfying the following Helmholtz equation (Kinsler et. al, 2000),

$$\nabla^2\phi + k^2\phi = 0 \qquad (2),$$

where $k = 2\pi f/c$ is the wave number and c is the speed of sound. At the inlet and the outlet section of the duct, a boundary condition of zero acoustic pressure was set. The computation grid consisted of 3-node linear 2-D acoustic triangular elements. The acoustic particle velocity associated with the first acoustic-mode of the duct, figure 3, was determined from the computed acoustic pressure field by using Euler's equation:

$$\rho \frac{\partial \vec{v}}{\partial t} = -\nabla p \qquad (3),$$

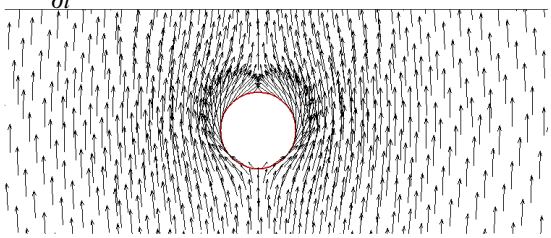

Figure 3: Vectors of the acoustic particle velocity around the cylinder taken at the maximum upward direction in the acoustic cycle.

3.3 Flow-Acoustic Coupling

In order to perform the triple product in equation (1), it is crucial to determine first the phase angle between the acoustic and the vortex shedding cycles. This phase relationship was obtained from the flow solver by monitoring the cross-flow oscillation at the boundaries and the lift force on the cylinder. Typical results are shown in figure 4 for the case of frequency coincidence, i.e. when the frequency of acoustic resonance is equal to the vortex shedding frequency, which was 486 Hz in this case. A phase shift of 162º was determined from figure 4. The coupling between the unsteady flow field and the acoustic field was therefore performed at this phase shift (162º) for a complete acoustic cycle.

It is important to mention that this coupling procedure is a one way coupling phenomenon, which means that the effect of resonant sound field on the flow is fully accounted for, but the excitation of the sound field by the flow is not considered. This approach does not affect the locations of the sound sources or sinks. The wake structure behind the cylinder after applying the cross-flow perturbation is shown in figure 5. A comparison between figure 2 and 5 shows that after applying the cross-flow perturbation, the vortex formation length decreases, which is similar to that reported for the case of forced oscillating cylinder. Moreover, by comparing the lift coefficient during lock-in, shown in figure 4, with that before applying the cross-flow oscillation, shown in figure 1, it is clear that the amplitude of the lift coefficient has increased to about 0.9.

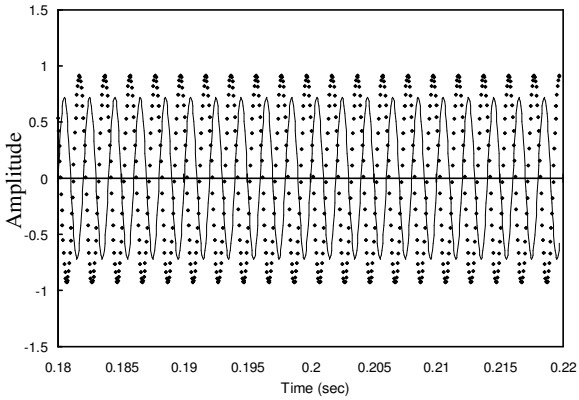

Figure 4: Phase relationship between the cross-flow oscillation and the lift coefficient on the cylinder. Solid line, cross-flow oscillation in m/s; ♦, lift force coefficient.

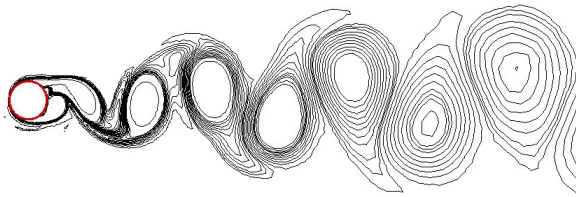

Figure 5: Vorticity contours behind a single cylinder at Re = 25000, after applying the cross-flow oscillation. The flow structure corresponds to the same time instant as that of figure 2.

The instantaneous acoustic power was calculated every 45º of the oscillation cycle. The total acoustic energy is the integration of the instantaneous acoustic power over a complete acoustic cycle and is calculated using equation (1). Figure 6 shows the vorticity and the instantaneous acoustic power taken when the acoustic particle velocity is at its maximum in the downward direction. Figure 7 shows the total acoustic energy over one cycle. The red colour in these figures represents net positive energy, or acoustic energy production, and the blue colour represents net negative, or absorbed, energy.

The total energy transfer per cycle at different downstream locations is shown in figure 8. For each streamwise location, the total energy represents the total energy integrated over a strip of the flow field with height $y = \pm 10\ D$ and a small width of Δx centered at the streamwise location. As it can be seen from this figure, the total energy transfer just downstream of the cylinder is positive and is larger than that occurring in the downstream region, which means that there is a strong acoustic

source located there, resulting in a net positive energy transfer from the flow field to the sound field. This can be illustrated further by calculating the cumulative sum of the total acoustic energy in the streamwise direction, which is shown in figure 9. It is clear from this figure that the total acoustic energy oscillates about a mean value that is established in a small region of about one diameter downstream of the cylinder.

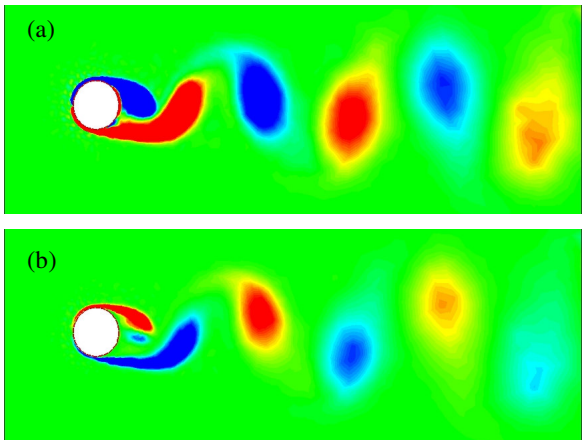

Figure 6: Contours of the vorticity field and the instantaneous acoustic power taken when the acoustic particle velocity is at its maximum in the downward direction. (a) vorticity contours; (b) instantaneous acoustic power.

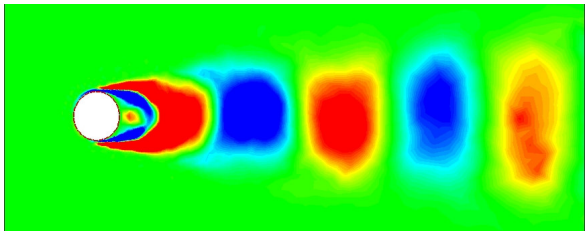

Figure 7: Total acoustic energy over one cycle.

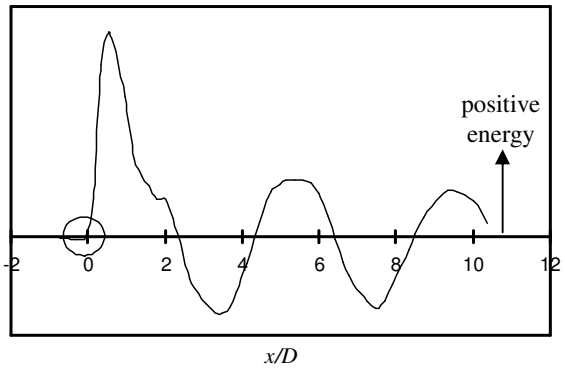

Figure 8: Total energy transfer per cycle at different downstream locations.

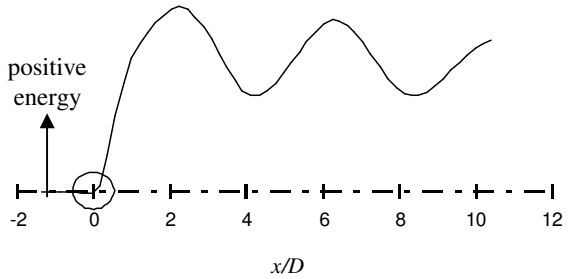

Figure 9: The cumulative sum of the total acoustic energy in the downstream direction.

4. TANDEM CYLINDERS RESULTS

The same numerical technique as that used in the case of a single cylinder was used here. The simulation of the flow was performed at a Reynolds number of 25000. Based on this Reynolds number, Strouhal number of vortex shedding is about 0.18. The wake structure behind the tandem cylinders before applying the cross-flow oscillation is shown in figure 10.

The same techniques as in section 3.2 are used here for the two tandem cylinders with a spacing ratio of L/D = 2.5 to calculate the acoustic particle velocity as shown in figure 11.

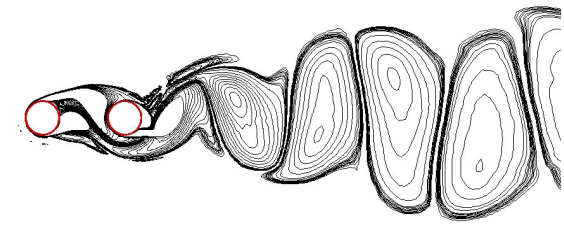

Figure 10: Vorticity contours behind two tandem cylinders, L/D = 2.5, at Re = 25000 before applying the cross-flow oscillation.

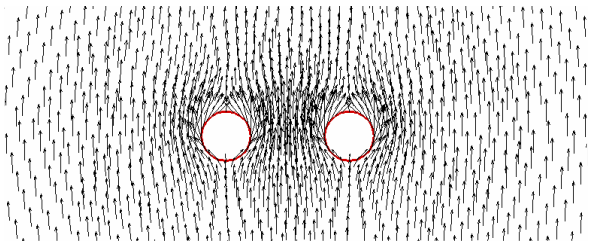

Figure 11: Vectors of the acoustic particle velocity around tandem cylinders taken at the maximum upward direction in the acoustic cycle.

4.1 Coincidence Acoustic Resonance

To simulate the coincidence acoustic resonance, the ratio between the forcing frequency of transverse oscillation, f_a, to that of the vortex shedding, f_v, was varied from about 0.9 to 0.8, and therefore the reduced velocity for this case was maintained in the range of 6 to 6.8, respectively.

Several oscillation amplitudes were simulated, however a minimum oscillation amplitude of about 10% of the main flow velocity was necessary to lock-in the vortex shedding frequency.

As in the case of the single cylinder, the phase relationship between the transverse oscillation and the vortex shedding cycle was monitored and the phase angle between the cross-flow oscillation and the fluctuating lift force on the downstream cylinder was found to be 225º. Therefore, the computation of the acoustic power (i.e. the triple product) was performed at this phase shift for a complete acoustic cycle.

Figure 12 shows contours of the total acoustic energy, and figure 13 shows the total energy transfer per cycle for different downstream locations. It is clear from this figure that there is an acoustic source located just downstream of the downstream cylinder. The energy transfer per cycle associated with this acoustic source is substantially high, which is similar to the case of a single cylinder. For the gap between the cylinders, there is production as well as absorption of acoustic energy and therefore the net effect of gap flow seems to cancel out, or becomes a small positive amount of energy transfer. Therefore, the coincidence acoustic resonance is excited primarily by the aeroacoustic source, which is concentrated in a small region of about one diameter downstream of the downstream cylinder. This is illustrated in figure 14, which shows the cumulative sum of the total acoustic energy in the streamwise direction. Thus, the excitation mechanism of the coincidence acoustic resonance seems similar to that of a single cylinder.

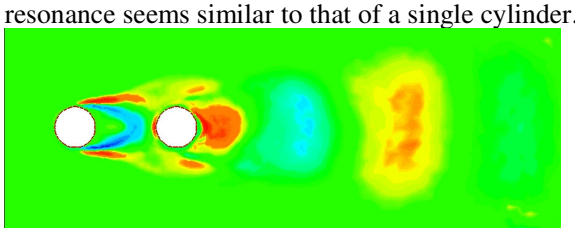

Figure 12: Total acoustic energy over one cycle for two tandem cylinders, L/D = 2.5, coincidence acoustic resonance, $f_a = 0.8\, f_v$.

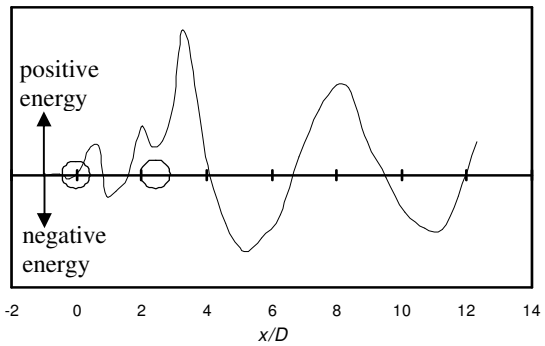

Figure 13: Total energy transfer per cycle for different downstream locations.

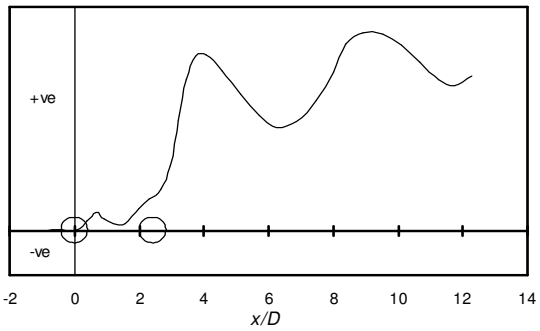

Figure 14: The cumulative sum of the total acoustic energy in the downstream direction.

4.2 Pre-coincidence Acoustic Resonance

To simulate the pre-coincidence acoustic resonance phenomenon, the frequency of the transverse oscillation was varied in a range corresponding to a reduced velocity range of 4 to 4.9. The amplitude of the transverse oscillation was varied until the vortex shedding frequency was locked-in to the forcing frequency. Only in the case with a frequency ratio of f_a/f_v = 1.2, the vortex shedding locked-into the excitation frequency with a minimum oscillation amplitude of 15% of the main flow velocity.

Examination of the phase relationship indicated that there is about 180º phase shift between the transverse oscillation and the lift force on the downstream cylinder. This phase angle was therefore imposed when computing the triple product to obtain the instantaneous acoustic power. Figure 15 shows contours of the total acoustic energy, and figure 16 shows the total energy transfer per acoustic cycle for different downstream locations. As it can be seen from these figures, a strong acoustic source in the flow field is located in the gap between the cylinders. The energy transfer from the flow field to the sound field associated with this acoustic source is dominant, as it can be seen clearly in figure 17. These results confirm the supposition that the acoustic source in the gap between the cylinders is the primary source generating the pre-coincidence acoustic resonance. This source is caused by the instability of the separated shear layers in the gap between the cylinders.

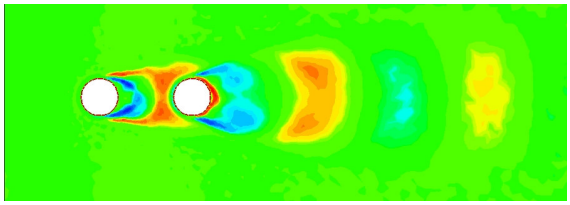

Figure 15: Total acoustic energy over one cycle for two tandem cylinders, L/D = 2.5, pre-coincidence acoustic resonance, $f_a = 1.2\, f_v$.

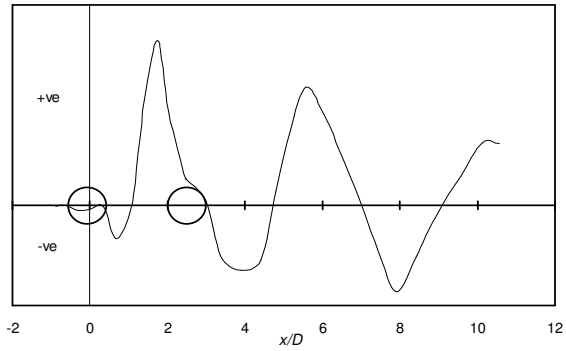

Figure 16: Total energy transfer per cycle for different downstream locations.

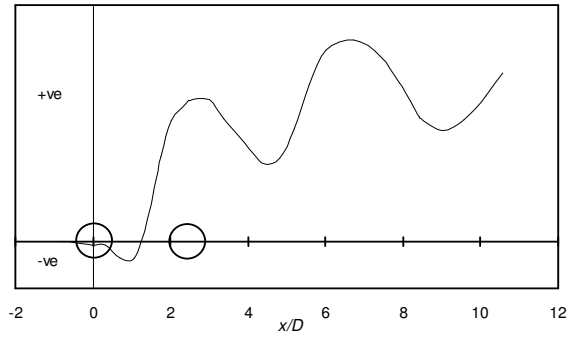

Figure 17: The cumulative sum of the total acoustic energy in the downstream direction.

5. CONCLUSIONS

A numerical simulation was performed to investigate the flow-excited acoustic resonance process for the case of a single cylinder and two tandem cylinders in cross-flow. The spacing ratio of the tandem cylinders was $L/D = 2.5$.

For the case of a single cylinder, there is an acoustic source located just downstream of the cylinder where a positive energy is transferred from the flow field to the sound field. This acoustic source is caused by the vortex shedding observed in the wake of the cylinders before the onset of acoustic resonance.

For the case of two tandem cylinders, two acoustic sources were found in the flow field. One of them is located in the gap between the cylinders and the other one is located just downstream of the downstream cylinder. For the coincidence acoustic resonance, the excitation mechanism is caused primarily by the downstream acoustic source, which is similar to the excitation mechanism of the single cylinder case. However, for the pre-coincidence acoustic resonance, the acoustic source in the gap is shown to be the major source of excitation.

6. REFERENCES

Blevins, R. D., 1985, The effect of sound on vortex shedding from cylinders. Journal of Fluid Mechanics, **161**: 217-237.

Howe M. S., 1975, Contributions to the theory of aerodynamic sound with application to engine jet noise and theory of the flute. Journal of Fluid Mechanics, **71**: 625 – 673.

Howe M. S., 1984, On the absorption of sound by turbulence and other hydrodynamic flows. IMA Journal of Applied Mathematics, **3**2: 187 – 209.

Hourigan K., Welsh M. C., Thompson M. C. and Stokes A. N., 1990, Areodynamic sources of acoustic resonance in a duct with baffles. Journal of Fluids and Structures, **4**: 345-370.

Hourigan K., A. N. Stokes, M. C. Thompson and M. C. Welsh, 1986, Flow induced acoustic resonances for a bluff body in a duct: a numerical study. 9th Australian fluid mechanics conference, Auckland, pp. 504-507.

Kinsler, L. E., Frey, A. R., Coppens, A. B. and Sanders, J. V., 2000, Fundamentals of acoustics, Fourth Edition, John Wiley and Sons, Inc.

Mohany, A. and Ziada, S., 2005, Flow excited acoustic resonance of two tandem cylinders in cross flow. Journal of Fluids and Structures, **21**: 103-119.

Mohany, A., 2006, Flow-sound interaction mechanisms of a single and two tandem cylinders in cross-flow. Ph.D. thesis, McMaster University.

Tan, B. T., Thompson M. C. and Hourigan K., 2003, Sources of acoustic resonance generated by flow around a long rectangular plate in a duct. Journal of Fluids and Structures, **18**: 729-740.

Saghafian, M., Stansby, P. K., Saidi, M. S. and Apsley, D. D., 2003, Simulation of turbulent flows around a circular cylinder using nonlinear eddy-viscosity modelling: steady and oscillatory ambient flows. Journal of Fluids and Structures, **17**: 1213-1236.

Stoneman S. A. T., Hourigan K., Stokes A. N. and Welsh M. C., 1988, Resonant sound caused by flow past two plates in tandem in a duct. Journal of Fluid Mechanics, **192**: 455-484.